Impaired inflammation resolution in murine bone marrow failure is rescued by Resolvin E1 treatment

Rachel Grazda[1]*, Allison N. Seyfried[1,4]*, Krishna Rao Maddipatti[2], Gabrielle Fredman[3], Katherine C. MacNamara[1#]

*co-first authors

[1]Department of Immunology and Microbiology, Albany Medical College, Albany, New York, USA;
[2]Department of Pathology, Lipidomics Core Facility, Wayne State University, Detroit, Michigan, USA;
[3]Department of Molecular and Cellular Physiology, Albany Medical College, Albany, New York, USA;
[4]Current address: Institute for Clinical Pharmacodynamics, Schenectady, NY, USA

[#] Corresponding author:
Katherine C. MacNamara
Department of Immunology and Microbial Disease
Albany Medical College, MC-151
47 New Scotland Avenue
Albany, NY 12208
Phone: 518-262-0921
Email: macnamk@mail.amc.edu

Running Title: **Resolvin E1 improves SAA**

Key Points:

- Deficiencies in efferocytosis during SAA are associated with expansion of MerTK^{hi} SIRPα^{hi} monocytes and increased CD47 expression.

- Imbalanced pro-inflammatory/pro-resolving lipid mediators correlated with SAA progression; RvE1 treatment improves efferocytosis and disease.

Abstract

Severe aplastic anemia (SAA) is an acquired form of bone marrow failure characterized by a profound loss of hematopoietic stem cells and failure to produce blood and immune cells. T cells are well-known drivers of disease, though underlying mechanisms causing persistent inflammation remain unknown. Typically, inflammation resolves via an active process mediated by specialized pro-resolving mediators (SPMs), such as resolvins. SPMs dampen inflammation without compromising host immunity, in part, through their ability to induce efficient clearance of apoptotic cells by phagocytes (i.e., efferocytosis). In a murine model of SAA, we identify a novel population of marrow monocytes that co-express the efferocytic receptor MerTK and the inhibitory receptor SIRPα. At the same time, the marrow contained a significant increase in apoptotic and dead cells that expressed the 'don't eat me' marker CD47. Myeloid cells from the marrow of SAA-induced mice exhibited reduced phagocytosis and efferocytosis, relative to controls. Consistent with impaired resolution responses, lipidomic analysis of the marrow revealed an imbalance of pro-inflammatory to pro-resolving lipid mediators. Specifically, we observed significantly reduced 18-hydroxyeicosapentaenoic acid (18-HEPE), a precursor to the E-series resolvins, followed by markedly increased prostaglandins and thromboxane in SAA. Treatment with exogenous Resolvin E1 (RvE1) increased BM cellularity, platelet count, and survival in SAA-induced mice, correlating with improved efferocytotic function. Our findings suggest that defective resolution pathways contribute to disease progression in SAA and demonstrate that SPMs, such as RvE1, may offer new strategies to treat disease that do not rely on immune suppression.

Word count: 244

Introduction

Idiopathic severe aplastic anemia (SAA) is a rare form of bone marrow failure (BMF) in which T cell-derived IFNγ and macrophage-derived tumor necrosis factor (TNF) drive the loss of hematopoietic stem and progenitor cells (HSPCs), resulting in pancytopenia.[1,2] Patients diagnosed with SAA have significantly increased interferon gamma (IFNγ) and TNF levels in the blood and BM.[3,4] Current therapies for SAA remain limited to immunosuppressive therapy (IST; anti-thymocyte globulin and cyclosporine) and BM transplantation.[5-7] Although the mechanism was unknown in 1981, treatment of patients with anti-thymocyte globulin in conjunction with BM transplantation increased survival odds immensely.[5]

Using IFNγ adenylate-uridylate–rich element (ARE)–deleted (del) mice, which exhibit increased IFNγ levels, Lin et al demonstrated that autoreactive T cells did not directly mediate destruction of HSCs during SAA, rather, IFNγ acted on the HSPC compartment to inhibit progenitor cell maturation and differentiation.[1] It has also been shown in a murine model of SAA induced by lymphocyte transfer, that TNF produced by host macrophages drives IFNγ production and infiltration of T cells into the BM during SAA.[2] Additionally, macrophages were shown to drive disease in an IFNγR- and CCR5-dependent manner.[8,9] Therefore, although T cells are an important target of current IST, additional cell types likely contribute to disease pathogenesis.

In 1995, researchers noted that patients with aplastic anemia exhibited an increased frequency of apoptotic $CD34^+$ progenitor cells in the BM, and the frequency of apoptotic cells correlated with severity of disease.[10] These data suggested that increased apoptosis of progenitors contributed to disease progression. In addition,

rampant cell death, driven by the Fas/FasL pathway for apoptosis, leads to the destruction of the hematopoietic stem and progenitor pool[11], as well as other cells[12]. Macrophages are critical for SAA progression, in part through producing and augmenting inflammatory mediators[2,8,9]. Macrophages are also important phagocytes within the BM, among other tissues, where they remove apoptotic cells[13,14], and promote tissue regeneration[15].

Efficient clearance of apoptotic and dead cells by phagocytes, termed efferocytosis, is crucial for inflammation-resolution and tissue function at homeostasis.[16] Apoptotic cells provide both “find me” and “eat me” signals to phagocytes[17], and phosphatidylserine (PS) is a well-known “eat me” signal recognized by tissue-resident phagocytes and efferocytic monocyte-derived macrophages.[18,19] Apoptotic signaling promotes rearrangement of the phospholipid bilayer to expose PS on the outer leaflet. Externalized PS is either recognized directly, or via the linker molecules Gas6 or Protein S, by TAM receptors on phagocytes such as MerTK. Signaling through MerTK induces cytoskeleton rearrangements that initiates engulfment of the apoptotic cell.[17,20] Efferocytic function is regulated, however, to prevent clearance of healthy cells. Indeed, healthy, viable cells express “don’t eat me” signals, such as CD47, that interact with inhibitory receptors expressed by phagocytes, such as SIRPα, resulting in the inhibition of phagocytosis.[21,22]

Resolution of inflammation is an active process mediated by a class of lipid mediators termed specialized pro-resolving mediators (SPMs).[23] SPMs, such as the D- and E-series resolvins, derived from omega-3 polyunsaturated fatty acids, possess potent pro-resolving actions and are essential for resolution.[23] Resolvin E1 (RvE1) has

been shown to improve efferocytosis in various inflammatory disease models such as periodontitis[24], colitis[25], lung cancer[26], acute lung injury and bacterial pneumonia[27], asthma[28], and atherosclerosis[29], to name a few. Using an established, preclinical murine model of SAA, we demonstrate dysfunctional inflammation resolution programs, as determined by impaired efferocytosis and an imbalance in pro-inflammatory and pro-resolving lipid mediators. We identify a unique population of MerTK^{hi} SIRPα^{hi} monocytes, and an accumulation of CD47^{+} apoptotic cells within the BM during SAA, that correlate with impaired cell clearance. RvE1 treatment, given to mice with established SAA, provided significant protection and improved efferocytosis. Our findings provide new insight to inflammation resolution programs and SAA pathogenesis. Moreover, our work offers key rationale to pursue novel therapeutic strategies to treat BMF that improve inflammation resolution without limiting host defense.

Methods

Mice: All animal protocols were approved by the Institutional Animals Care and Use Committee at Albany Medical College. C57BL/6 ($H^{b/b}$) and BALB/cAnN ($H\text{-}2^{d/d}$) mice were purchased from Taconic (Albany, NY, https://www.taconic.com/). Macrophage insensitive to IFNγ (MIIG) mice were generously gifted by Dr. Michael Jordan. Hybrid B6 F1 ($H\text{-}2^{b/d}$) mice were generated by crossing C57BL/6 or MIIG mice on a C57BL/6 background with BALB/c mice. All mice were bred and housed in the Animal Resource Facility under microisolator conditions at Albany Medical College.

Bone Marrow Failure Induction: A splenocyte-infusion method was used to induce bone marrow failure (BMF) in Hybrid F1 mice aged 6-9 weeks. Hybrid F1 mice were subjected to sub-lethal radiation (300 RADs) using a ^{137}Cs source. Irradiated mice received adoptive transfer of 6.5×10^6 C57BL/6 splenocytes from age- and gender-matched donors via intraperitoneal injection. Mice were euthanized via CO_2 inhalation followed by cervical dislocation.

Blood Collection and CBCs: Blood was collected from euthanized mice into EDTA-coated tubes via cardiac puncture and analyzed with a Heska Element HT5 for complete blood count (CBC).

Cell Preparation and Flow Cytometry: Whole bone marrow was flushed from femurs and tibias. After RBC lysis, cell suspensions were plated and stained. See supplemental

Table 1 for antibody details. Data were collected using a FACSymphony A3 (BD Biosciences) with FACSDiva software or Cytek Northern Light (Cytek Bioscienes) with SpectroFlo software and analyzed using FlowJo software (TreeStar, Ashland, OR).

Phagocytosis Assay: 200µL fluorescent DiI ($DiIC_{18}(3)$)-labeled liposomes (Liposoma) were administered to mice via retro-orbital I.V. injection on day 9 post induction. BM and blood was harvested 16 hours post injection.

Efferocytosis Assay: Whole BM was flushed and incubated with phosphatidylserine (PS)-coated lipid microparticles (Echelon Biosciences) for 1 hour at 37°C. Cells were then stained for flow cytometry.

SIRPα Neutralization: Anti-SIRPα (clone P84; 200 µg; BioXCell) antibody was diluted in PBS and administered to mice via intraperitoneal injection on days 7 and 9 post-induction for day 10 harvest, or days 7, 9, 11, and 13 for day 14 harvest.

RvE1 Treatment: Resolvin E1 (250ng; Cayman Chemical) was diluted in PBS and administered to mice via intraperitoneal injection on days 7, 9, 11 for day 12 harvest, or days 7, 9, 11, and 13 for day 14 harvest.

Gene Expression: Whole BM was flushed and pooled from hind limbs of three mice per group. RBCs were lysed and cells were stained to sort purified monocytes (SSC^{low}, $CD11b^{+}$, $Ly6C^{hi}$, $Ly6G^{-}$). Monocytes were collected in RLT lysis buffer (Qiagen). mRNA

was isolated (Qiagen RNeasy Mini Kit) and quantitative-RT-PCR was performed (Eppendorf *realplex*^{2} Mastercycler).

Protein analysis: Whole BM was flushed from the pelvis. BM cell lysates were homogenized manually with a pestle in a buffer containing IGEPAL CA-630 and protease inhibitors. Soluble Mer and Gas6 were quantified using ELISA kits from Ray Biotech (accession #Q60805 and Q61592, respectively) and normalized to whole protein using the Pierce BCA protein assay kit (Thermo Fisher, catalog #23255).

Lipidomic analysis: Whole BM was flushed from mouse hind limbs (femurs and tibias) with ice cold PBS. Samples were flash frozen on dry ice before shipment to Wayne State University Lipidomics Core facility for analysis. Fatty acyl lipidomic analysis was performed as per published procedures.[30,31] Briefly, the frozen samples were thawed on ice at the time of analysis, and homogenized using Zirconium beads (Precellys, Biotage). The homogenate was extracted for fatty acyl lipids using StrataX columns (Phenomenex) following supplementation with internal standards. The extracts were analyzed by LC-MS/MS using Multiple Reaction Monitoring (MRM) method on a QTRAP5500 mass analyzer (Sciex). Identities of the individual lipid mediators were confirmed from the retention times and spectra recorded for each detected peak and were quantified relative to the internal standards. The data were normalized against protein content of the samples (ng/mg protein).

Survival Studies: PBS or 250 ng RvE1 was administered via intraperitoneal injection days 7, 9, 11, and 13 post induction. Mice were monitored twice daily for 28 or 37 days and euthanized when moribund. Euthanasia criteria was based on signs of dehydration, response to physical stimuli, and mobility — as previously described.[9]

Statistical Analysis: Data were analyzed with GraphPad Prism software (version 8.0, La Jolla, CA). Statistical analysis was performed using two-tailed Student's T-test or Two-Way ANOVA with Tukey's post-hoc analysis, and details are provided in each figure legend. Lipidomic data was analyzed using GraphPad Prism software (version 9.0, La Jolla, CA). Principal component analysis was performed using 22 lipid mediators detected across all samples from mice 3 days post-radiation for healthy (no radiation), radiation controls, and SAA-induced mice. Data were standardized and principal components were selected using Kaiser-Guttman's rule. Heat map analysis was performed on LC-MS/MS data from radiation controls and SAA-induced mice, normalized to healthy controls.

All methods for flow cytometric analysis and lipidomic analysis are described in detail in the supplemental materials (available on the Blood website), and data will be made available upon request.

Results

Monocytosis, cytopenias, and increased marrow cell death during SAA

Thrombocytopenia and decreased BM cellularity are well-known characteristics of severe aplastic anemia (SAA).[1,8,9] Using a murine model of SAA induced by adoptive transfer of splenocytes to sub-lethally irradiated F1 mice[8,32,33], we observed a significant decrease in red blood cells (**Figure 1A**) and platelets (**Figure 1B**) by 10 days post splenocyte transfer (dpst). We also observed a dramatic loss of blood lymphocytes correlating with an expansion of the circulating blood monocyte population (**Figure 1C**). Mice induced to develop SAA exhibited significant hypocellularity by 10 dpst (**Figure 1D**), though BM monocytes ($CD11b^{+}Ly6C^{hi}Ly6G^{-}$) were increased by both frequency and number, whereas neutrophils ($CD11b^{+}$ $Ly6C^{low}$ $Ly6G^{hi}$) were decreased (**Figure 1E-F;** supplemental Fig. 1A-B). Therefore, disease progression is associated with a hematopoietic program that favors monopoiesis.

To investigate cell death during disease progression we performed Annexin V and 7-AAD staining (**Figure 1G**). Similar frequencies of apoptotic ($AnnV^{+}7\text{-}AAD^{-}$) and dead cells were observed between radiation controls and SAA-induced mice at 8 dpst (**Figure 1H**). However, by 10 dpst the SAA-induced mice had a striking increase in dead ($7\text{-}AAD^{+}$) cells, compared to radiation controls. IFNγ can induce apoptosis[34] and is a known driver of disease. We previously demonstrated that transgenic mice containing macrophages insensitive to IFNγ (referred to as MIIG mice[8]) exhibit protection from SAA. Here we observed that SAA-induced MIIG mice exhibited a decrease in the frequency of dead cells, relative to littermate control (LC) counterparts (supplemental

Fig. 2). These data suggest that the accumulation of dead cells and increased monocytes, during the early stages of SAA, correlate with disease progression.

Increased surface expression of MerTK and SIRPα on monocytes during SAA

Under healthy conditions, apoptotic cells are rapidly cleared, and the accumulation of dead cells during SAA suggested that efferocytosis may be impaired. Monocytes and macrophages (MΦs) are the main efferocytes within the BM[35], and MerTK is a critical receptor for efferocytosis that, when bound to PS on apoptotic cells, initiates cytoskeletal rearrangement and the subsequent uptake of dead or dying cells.[36] We hypothesized that reduced MerTK expression or cleavage via ADAM17, may contribute to impaired clearance of dead cells in the marrow during SAA. To address this, we performed flow cytometry to evaluate MerTK expression on myeloid cells 10 days post SAA induction. In contrast to our prediction, the frequency and absolute number of MerTK expressing monocytes expanded dramatically in the BM of SAA mice (**Figure 2A-C**). MerTK expression on macrophages also increased during SAA, though these changes were not statistically significant (supplemental Fig. 3A-C). Analysis of monocyte gene expression indicated an increase in *Mertk*, as well as *Ifnγ* and *Tnf* (known drivers of disease)[1,2], in SAA mice, relative to radiation controls (supplemental Fig. 4 A-C).

Under inflammatory conditions, MerTK can be cleaved by ADAM17[37], releasing soluble Mer (sMer) into the extracellular milieu to act as a decoy for Gas6 and Protein S.[38] Under SAA conditions, we observed increased Mer in BM homogenates (BM-H), though this did not reach statistical significance (supplemental Fig. 4D). To complement

this analysis, we also measured Gas6 in the marrow and found a significant decrease in SAA mice, relative to radiation control (supplemental Fig. 4E). These data suggest that, during SAA, increased Mer cleavage without sufficient production and secretion of Gas6 may contribute to impaired efferocytosis, and the subsequent accumulation of dead and dying cells.

Healthy cells can actively suppress their engulfment via “don’t eat-me” signaling, such as the CD47-SIRPα axis. We found that the population of monocytes with high MerTK expression during SAA also exhibited a significant increase in SIRPα expression, resulting in a striking increase in the absolute number of MerTK^{hi} SIRPa^{hi} monocytes **(Figure 2D-F**). We also observed an increase in SIRPα on MerTK^{hi} macrophages (supplemental Fig. 3D-F). Together, these data suggest that, under SAA conditions, monocytes are primed for efferocytosis but expression of SIRPα may impair this function. Monocytes from MIIG mice expressed significantly reduced MerTK and SIRPα, correlating with resistance of MIIG mice to SAA progression (supplemental Fig. 5). Taken together, our data are consistent with a role of aberrantly high MerTK expression and the unique population of MerTK^{hi} SIRPα^{hi} monocytes in disease pathogenesis.

Increased CD47 expression on dead cells

CD47 is an important marker of “self” for healthy viable cells, and apoptotic cells lose expression of CD47 enabling phagocytic clearance.[39,40] During SAA, however, we observed increased CD47 expression on both live and apoptotic BM cells (**Figure 2G-I**).

These data suggest that increased CD47 on apoptotic cells, combined with increased SIRPα^{hi} monocytes, may prevent efficient clearance in the marrow during SAA.

To better understand whether the SIRPα–CD47 axis contributes to disease, SAA-induced mice were treated with anti-SIRPα neutralizing antibody days 7, 9, and 11 post induction (supplemental Fig. 6A). Although we did observe a significant decrease in the frequency of dead cells and CD47^{+} apoptotic cells (supplemental Fig. 6C-D), anti-SIRPα treatment exacerbated anemia during SAA by 14 dpst (supplemental Fig. 6F-I). Together, these data support the idea that the SIRPα–CD47 axis contributes to the accumulation of dead cells during SAA, but as this axis is necessary for RBC circulation[41], we reasoned it would not be an effective therapeutic target in SAA.

Decreased phagocytosis and efferocytosis in SAA

To examine whether phagocytes were functionally impaired during SAA, F1 mice were induced to develop disease and administered fluorescently-labeled (Dil-labeled) liposomes day 9 post-induction to evaluate phagocytotic capacity. BM was harvested day 10 to evaluate the uptake of liposomes via flow cytometry (supplemental Fig. 7A). SAA mice exhibited a decrease in Dil liposome-positive F4/80^{+} and CD11b^{+} cells, suggesting impairments in phagocytosis (supplemental Fig. 7B-E).

To better address whether efferocytosis is defective during SAA, we utilized phosphatidylserine (PS)-coated microparticles to mimic apoptotic cells. BM from SAA-induced mice and radiation controls was incubated with fluorescently tagged PS-coated lipid microparticles (PS-MPs), and uptake was determined via flow cytometry (**Figure 3A-B**). We observed a significant reduction in PS-MP^{+} monocytes and F4/80^{+} cells in

marrow isolated from SAA-induced mice, relative to controls, at 8 dpst (**Figure 3C-F**). Consistent with the role of impaired efferocytosis in disease progression, SAA-induced MIIG mice did not exhibit a significant decrease in PS-MPs, as compared to LC counterparts (supplemental Fig. 8). Together, these data demonstrate that during SAA progression, myeloid cells exhibit reduced phagocytosis and efferocytosis.

Imbalance of lipid mediators that regulate inflammation resolution in SAA

Based on our observation that efferocytosis is impaired during SAA progression, we next addressed how key resolution programs may be impacted in disease. To examine the lipid mediators associated with disease initiation and progression we performed LC-MS/MS to analyze the polyunsaturated fatty acid (PUFA) metabolome in BM of healthy, radiation control, and SAA-induced mice. Principal component analysis (PCA) revealed that a majority of the variation (PC1; 43%) at day 3 post-radiation was due to differences in mono-hydroxy eicosapentaenoic acids, including a decrease in 18-HEPE in SAA mice, relative to radiation controls (**Figure 4A,** supplemental Fig. 9A). Indeed, limited 18-HEPE, the precursor to the E-series resolvins, may contribute to impaired generation of these SPMs in the marrow during SAA (**Figure 4B**). By day 8, SAA-induced mice had significantly elevated PGE2, PGD2, and TXB2 relative to radiation controls (**Figure 4C-E,** supplemental Fig. 9B, supplemental Table 2). Our data suggest that in the context of SAA, omega-3 derived lipid precursors are decreased in the marrow. Together, these data demonstrate that SAA pathogenesis correlates with unregulated prostanoid and thromboxane synthesis supporting our conclusion that resolution kinetics are defective.

Resolvin E1 provides therapeutic benefit in SAA

To address whether SPMs may be viable therapeutic targets in mitigating the pathogenesis of SAA, we first examined expression of key SPM receptors on BM monocytes. We determined by flow cytometry that ChemR23, the receptor for RvE1[42], was significantly upregulated on BM monocytes and neutrophils, but not on macrophages or LK cells (supplemental Fig. 10), which provided rationale for treating mice with exogenous RvE1.

To directly test the therapeutic efficacy of exogenous RvE1, we administered RvE1 or vehicle every other day, beginning at day 7 post-induction, a time point when marrow is hypocellular (**Figure 5A**). RvE1 treatment did not improve lymphopenia or anemia, or limit SAA-induced monocytosis (**Figure 5B**-**C**), however, a significant increase in circulating white blood cells and platelets was noted by 14 dpst (**Figure 5D-E**). Although not significant, we also observed increased overall BM cellularity by day 14 (**Figure 5F**). The number of BM monocytes remained unchanged; however, neutrophil numbers, total LK cells, and HSC progenitor populations were increased with RvE1 treatment (**Figure 5G-H;** supplemental Fig. 11). Moreover, we observed that RvE1 significantly improved survival when mice were administered therapeutic doses of RvE1, on days 7, 9, 11, and 13 post-SAA induction (**Figure 5I**).

Consistent with a role for RvE1 in improving resolution of inflammation, we observed that RvE1 treatment decreased expression of the inhibitory receptor SIRPα, (**Figure 6A**), which correlated with increased PS-MP^{+} monocytes and F4/80^{+} cells by 12

dpst (**Figure 6B-E**). Together, our data suggest that RvE1 therapy improves efferocytic function and bone marrow cellularity, which rescued disease. Moreover, these studies define a novel approach to treat autoimmune marrow failure.

Discussion

Efferocytosis is a crucial component of resolution pathways and maintains tissue homeostasis by limiting inflammation. By engaging in specific ligand-receptor signaling, such as PS and MerTK, efferocytes promote the resolution of inflammation by clearing dying cells, releasing anti-inflammatory mediators like IL-10 and TGF-β, and driving SPM biosynthesis.[20,37] Apoptotic cells that are not properly cleared enter secondary necrosis, characterized by the breakdown of the cellular membrane and the leakage of inflammatory DAMPs that may exacerbate inflammation.[20] Although impairments in resolution are known to underly several chronic inflammatory diseases[43-46], whether resolution responses are impaired during SAA or in other BMF diseases has yet to be investigated.

Here we find an increase in the frequency of dead and dying cells within the BM of SAA mice. While it is known that SAA is associated with increased apoptosis, the accumulation of necrotic cells also suggested deficiencies in cell clearance. The increase in dead and dying cells correlated with the expansion of a unique population of SIRPα^{hi} MerTk^{hi} monocytes, not observed in radiation controls. Indeed, IFNγ is known to drive monopoiesis[47], and earlier studies demonstrated that increased monocytes preceded the accumulation of macrophages in the bone marrow during SAA pathogenesis.[8] Consistent with a potential role of SIRPα^{hi} MerTk^{hi} monocytes in driving disease, we noted that this population was significantly reduced in the MIIG mouse model, a strain that is protected from developing SAA.[8] We reasoned that although the monocytes highly expressed the efferocytic receptor MerTK, they were likely impaired in efferocytic function due to co-expression of SIRPα, an inhibitory receptor.

Why MerTK expression is increased so strikingly requires further investigation, though our data suggests that MerTK expression is driven by IFNγ during SAA. The pathways necessary to initiate inflammation are also thought to program resolution[48,49], and induction of *Mertk* expression may be one mechanism whereby IFNγ, typically associated with acute inflammation, also participates in resolution. It is also known that under inflammatory conditions MerTK is susceptible to cleavage by ADAM17, generating soluble Mer (sMer).[50] The cleavage of MerTK is known to limit SPM biosynthesis and recent studies in atherosclerosis demonstrated that increased MerTK cleavage resulted in defective efferocytosis and disease progression.[37,51] Notably, sMer can antagonize full-length Mer by binding to and sequestering the ligand Gas6 and inhibiting Gas-mediated MerTK activation.[38] Our observation that SAA mice exhibited a slight increase in sMer and a decrease in Gas6 in the marrow compared to radiation controls, suggests that sMer may be contributing to improper MerTK activation and deficiencies in resolution responses.

Healthy viable cells can expose PS under normal physiological conditions. To prevent improper engulfment by phagocytes, healthy cells utilize “don’t eat me” markers, such as CD47. Dying cells typically lose or alter the expression of CD47 to enable cell clearance, as in the case of aging RBCs, where CD47 is expressed on normal RBCs, preventing their elimination by phagocytes.[41] Therefore, it is of no surprise that anti-SIRPα therapy worsened anemia in SAA-induced mice. High CD47 expression on dying cells has also been shown to promote inefficient clearance via the “nibbling” of cells, rather than whole-cell engulfment by phagocytes.[43] TNF and IFNγ, which are increased during SAA[2], have been shown to upregulate CD47

expression.[52,53] As defective efferocytosis is known to elicit pro-inflammatory cytokines, it is possible that CD47, TNF, and IFNγ play a critical role in the feedback loop that inhibits cellular clearance and inflammation-resolution, thus potentiating inflammation.

Specialized pro-resolving mediators (SPMs) actively drive the resolution of inflammation and a return to homeostasis.[23] Class switching of lipid mediators, from pro-inflammatory to pro-resolving, is essential for resolution to occur.[54] Lipid mediator analysis of the BM from SAA-induced mice demonstrated an imbalance of pro-inflammatory to pro-resolving mediators with exuberant prostanoid synthesis. SPM biosynthesis occurs via transcellular mechanisms that require close contact of cells expressing distinct enzymes, and it is notable that during SAA the bone marrow becomes increasingly hypocellular, which may prevent SPM generation. A loss of proper SPM biosynthesis or signaling has been linked with the exacerbation of inflammation in various disease settings.[55-57] While the cause is still unclear, a lack of SPM production and an increase in prostanoid synthesis, combined with dysregulated unalamation[58], appears to be contributing to persistent inflammation observed during SAA. A recent report uncovered a prostanoid storm limited efferocytosis in vitro and in atherosclerotic plaques[59], thus supporting the notion that sustained elevated prostanoids, without a compensatory increase in SPMs, may contribute to defective efferocytosis in the bone marrow during SAA.

Treatment with exogenous SPMs has been utilized to improve resolution in multiple experimental settings.[25,45,60] SPMs have a unique safety profile since they, unlike immunosuppressive therapies, do not compromise the host's natural immune response.[27,61] During SAA, 18-HEPE, the precursor for the E-series resolvins is

significantly reduced, relative to radiation controls. Meanwhile, the receptor for RvE1, ChemR23, was increased on monocytes and neutrophils in SAA. Together, these data suggested that RvE1 could be an ideal therapeutic for treating SAA. Indeed, RvE1 therapy, starting at a timepoint where the BM is already hypocellular, improved platelet count, BM cellularity, survival, and efferocytosis (**Figure 7**).

Current treatments for SAA rely on HSC transplantation, when possible, and IST, though IST has a high refractory rate and hinders the patient's natural immune response. Recently approved Etrombopag, an agonist of the thrombopoietin receptor, has shown improved response times in combination with IST, although, overall responses were not improved in older patients or those that began treatment with severe disease.[62] Recent preclinical studies using the Janus kinase (Jak1/2) inhibitor Ruxolitinib (Rux) demonstrated effectiveness in a murine model of SAA with markedly reduced T lymphocytes in the marrow.[63] However, toxicity associated with Rux use has been noted in humans and mouse models.[64,65] Therefore, improved therapeutic strategies are still needed for durable treatment of SAA. Our findings that efferocytosis was impaired in SAA, and that SPM therapy was efficacious, provide strong rationale for targeting inflammation-resolution during BM failure. Therapies aimed at improving resolution, perhaps in conjunction with lower dosing of IST, may provide a more effective and safe treatment for SAA that does not compromise the patient's natural immune response.

Word count: 3941

456

Acknowledgements

The authors would like to thank Jesse Bonin for technical assistance. This work was supported by CDMRP Bone Marrow Failure Research Program-IDA (BM190079) to K.C.M. This study was also supported in part by National Center for Research Resources, National Institutes of Health Grant S10RR027926 (K.R.M.)

Authorship

R.G. and A.N.S. performed *in vivo* experiments, analyzed data, and prepared figures. R.G. wrote the manuscript. K.R.M. provided oversight and guidance for LC-MS/MS studies and analyzed data. G.F. contributed to experimental design and data analysis for the project. K.C.M. conceived of the project, analyzed data, and wrote the manuscript. The order of the first authors was determined on the basis of the effort and contributions to writing of the manuscript.

Conflict-of-interest disclosure: The authors declare no competing financial interests.

References

1. Lin FC, Karwan M, Saleh B, et al. IFN-gamma causes aplastic anemia by altering hematopoietic stem/progenitor cell composition and disrupting lineage differentiation. *Blood*. Dec 11 2014;124(25):3699-708. doi:10.1182/blood-2014-01-549527
2. Sun W, Wu Z, Lin Z, et al. Macrophage TNF-alpha licenses donor T cells in murine bone marrow failure and can be implicated in human aplastic anemia. *Blood*. Dec 27 2018;132(26):2730-2743. doi:10.1182/blood-2018-05-844928
3. Zoumbos NC, Gascon P, Djeu JY, Young NS. Interferon is a mediator of hematopoietic suppression in aplastic anemia in vitro and possibly in vivo. *Proc Natl Acad Sci U S A*. Jan 1985;82(1):188-92. doi:10.1073/pnas.82.1.188
4. Merli P, Quintarelli C, Strocchio L, Locatelli F. The role of interferon-gamma and its signaling pathway in pediatric hematological disorders. *Pediatr Blood Cancer*. Apr 2021;68(4):e28900. doi:10.1002/pbc.28900
5. Gratwohl A, Osterwalder B, Nissen C, et al. [Treatment of severe aplastic anemia]. *Schweiz Med Wochenschr*. Oct 10 1981;111(41):1520-2. Behandlung der schweren aplastischen Anamie.
6. Xu L, Fu B, Wang W, et al. Haploidentical hematopoietic cell transplantation for severe acquired aplastic anemia: a case-control study of post-transplant cyclophosphamide included regimen vs. anti-thymocyte globulin & colony-stimulating factor-based regimen. *Sci China Life Sci*. Jun 2020;63(6):940-942. doi:10.1007/s11427-019-9585-x
7. Rosenfeld S, Follmann D, Nunez O, Young NS. Antithymocyte globulin and cyclosporine for severe aplastic anemia: association between hematologic response and long-term outcome. *JAMA*. Mar 5 2003;289(9):1130-5. doi:10.1001/jama.289.9.1130
8. McCabe A, Smith JNP, Costello A, Maloney J, Katikaneni D, MacNamara KC. Hematopoietic stem cell loss and hematopoietic failure in severe aplastic anemia is driven by macrophages and aberrant podoplanin expression. *Haematologica*. Sep 2018;103(9):1451-1461. doi:10.3324/haematol.2018.189449
9. Seyfried AN, McCabe A, Smith JNP, Calvi LM, MacNamara KC. CCR5 maintains macrophages in the bone marrow and drives hematopoietic failure in a mouse model of severe aplastic anemia. *Leukemia*. Nov 2021;35(11):3139-3151. doi:10.1038/s41375-021-01219-z
10. Philpott NJ, Scopes J, Marsh JC, Gordon-Smith EC, Gibson FM. Increased apoptosis in aplastic anemia bone marrow progenitor cells: possible pathophysiologic significance. *Exp Hematol*. Dec 1995;23(14):1642-8.
11. Liu CY, Fu R, Wang HQ, et al. Fas/FasL in the immune pathogenesis of severe aplastic anemia. *Genet Mol Res*. May 30 2014;13(2):4083-8. doi:10.4238/2014.May.30.3
12. Gupta P, Niehans GA, LeRoy SC, et al. Fas ligand expression in the bone marrow in myelodysplastic syndromes correlates with FAB subtype and anemia, and predicts survival. *Leukemia*. Jan 1999;13(1):44-53. doi:10.1038/sj.leu.2401233

13. Michalski MN, Koh AJ, Weidner S, Roca H, McCauley LK. Modulation of Osteoblastic Cell Efferocytosis by Bone Marrow Macrophages. *J Cell Biochem*. Dec 2016;117(12):2697-2706. doi:10.1002/jcb.25567

14. McCauley LK, Dalli J, Koh AJ, Chiang N, Serhan CN. Cutting edge: Parathyroid hormone facilitates macrophage efferocytosis in bone marrow via proresolving mediators resolvin D1 and resolvin D2. *J Immunol*. Jul 1 2014;193(1):26-9. doi:10.4049/jimmunol.1301945

15. Wynn TA, Vannella KM. Macrophages in Tissue Repair, Regeneration, and Fibrosis. *Immunity*. Mar 15 2016;44(3):450-462. doi:10.1016/j.immuni.2016.02.015

16. Doran AC, Yurdagul A, Jr., Tabas I. Efferocytosis in health and disease. *Nat Rev Immunol*. Apr 2020;20(4):254-267. doi:10.1038/s41577-019-0240-6

17. Elliott MR, Koster KM, Murphy PS. Efferocytosis Signaling in the Regulation of Macrophage Inflammatory Responses. *J Immunol*. Feb 15 2017;198(4):1387-1394. doi:10.4049/jimmunol.1601520

18. Shiratsuchi A, Osada S, Kanazawa S, Nakanishi Y. Essential role of phosphatidylserine externalization in apoptosing cell phagocytosis by macrophages. *Biochem Biophys Res Commun*. May 19 1998;246(2):549-55. doi:10.1006/bbrc.1998.8663

19. Fadok VA, Voelker DR, Campbell PA, Cohen JJ, Bratton DL, Henson PM. Exposure of phosphatidylserine on the surface of apoptotic lymphocytes triggers specific recognition and removal by macrophages. *J Immunol*. Apr 1 1992;148(7):2207-16.

20. Korns D, Frasch SC, Fernandez-Boyanapalli R, Henson PM, Bratton DL. Modulation of macrophage efferocytosis in inflammation. *Front Immunol*. 2011;2:57. doi:10.3389/fimmu.2011.00057

21. Gardai SJ, McPhillips KA, Frasch SC, et al. Cell-surface calreticulin initiates clearance of viable or apoptotic cells through trans-activation of LRP on the phagocyte. *Cell*. Oct 21 2005;123(2):321-34. doi:10.1016/j.cell.2005.08.032

22. Okazawa H, Motegi S, Ohyama N, et al. Negative regulation of phagocytosis in macrophages by the CD47-SHPS-1 system. *J Immunol*. Feb 15 2005;174(4):2004-11. doi:10.4049/jimmunol.174.4.2004

23. Serhan CN, Levy BD. Resolvins in inflammation: emergence of the pro-resolving superfamily of mediators. *J Clin Invest*. Jul 2 2018;128(7):2657-2669. doi:10.1172/JCI97943

24. Hasturk H, Kantarci A, Ohira T, et al. RvE1 protects from local inflammation and osteoclast- mediated bone destruction in periodontitis. *FASEB J*. Feb 2006;20(2):401-3. doi:10.1096/fj.05-4724fje

25. Ishida T, Yoshida M, Arita M, et al. Resolvin E1, an endogenous lipid mediator derived from eicosapentaenoic acid, prevents dextran sulfate sodium-induced colitis. *Inflamm Bowel Dis*. Jan 2010;16(1):87-95. doi:10.1002/ibd.21029

26. Kantarci A, Kansal S, Hasturk H, Stephens D, Van Dyke TE. Resolvin E1 Reduces Tumor Growth in a Xenograft Model of Lung Cancer. *Am J Pathol*. Oct 2022;192(10):1470-1484. doi:10.1016/j.ajpath.2022.07.004

27. Seki H, Fukunaga K, Arita M, et al. The anti-inflammatory and proresolving mediator resolvin E1 protects mice from bacterial pneumonia and acute lung injury. *J Immunol*. Jan 15 2010;184(2):836-43. doi:10.4049/jimmunol.0901809

28. Haworth O, Cernadas M, Yang R, Serhan CN, Levy BD. Resolvin E1 regulates interleukin 23, interferon-gamma and lipoxin A4 to promote the resolution of allergic airway inflammation. *Nat Immunol*. Aug 2008;9(8):873-9. doi:10.1038/ni.1627

29. Hasturk H, Abdallah R, Kantarci A, et al. Resolvin E1 (RvE1) Attenuates Atherosclerotic Plaque Formation in Diet and Inflammation-Induced Atherogenesis. *Arterioscler Thromb Vasc Biol*. May 2015;35(5):1123-33. doi:10.1161/ATVBAHA.115.305324

30. Norris PC, Skulas-Ray AC, Riley I, et al. Identification of specialized pro-resolving mediator clusters from healthy adults after intravenous low-dose endotoxin and omega-3 supplementation: a methodological validation. *Sci Rep*. Dec 21 2018;8(1):18050. doi:10.1038/s41598-018-36679-4

31. Maddipati KR, Romero R, Chaiworapongsa T, et al. Eicosanomic profiling reveals dominance of the epoxygenase pathway in human amniotic fluid at term in spontaneous labor. *FASEB J*. Nov 2014;28(11):4835-46. doi:10.1096/fj.14-254383

32. Chen J, Lipovsky K, Ellison FM, Calado RT, Young NS. Bystander destruction of hematopoietic progenitor and stem cells in a mouse model of infusion-induced bone marrow failure. *Blood*. Sep 15 2004;104(6):1671-8. doi:10.1182/blood-2004-03-1115

33. Bloom ML, Wolk AG, Simon-Stoos KL, Bard JS, Chen J, Young NS. A mouse model of lymphocyte infusion-induced bone marrow failure. *Exp Hematol*. Dec 2004;32(12):1163-72. doi:10.1016/j.exphem.2004.08.006

34. Ossina NK, Cannas A, Powers VC, et al. Interferon-gamma modulates a p53-independent apoptotic pathway and apoptosis-related gene expression. *J Biol Chem*. Jun 27 1997;272(26):16351-7. doi:10.1074/jbc.272.26.16351

35. Poon IK, Lucas CD, Rossi AG, Ravichandran KS. Apoptotic cell clearance: basic biology and therapeutic potential. *Nat Rev Immunol*. Mar 2014;14(3):166-80. doi:10.1038/nri3607

36. Scott RS, McMahon EJ, Pop SM, et al. Phagocytosis and clearance of apoptotic cells is mediated by MER. *Nature*. May 10 2001;411(6834):207-11. doi:10.1038/35075603

37. Cai B, Thorp EB, Doran AC, et al. MerTK cleavage limits proresolving mediator biosynthesis and exacerbates tissue inflammation. *Proc Natl Acad Sci U S A*. Jun 7 2016;113(23):6526-31. doi:10.1073/pnas.1524292113

38. Sather S, Kenyon KD, Lefkowitz JB, et al. A soluble form of the Mer receptor tyrosine kinase inhibits macrophage clearance of apoptotic cells and platelet aggregation. *Blood*. Feb 1 2007;109(3):1026-33. doi:10.1182/blood-2006-05-021634

39. Lv Z, Bian Z, Shi L, et al. Loss of Cell Surface CD47 Clustering Formation and Binding Avidity to SIRPalpha Facilitate Apoptotic Cell Clearance by Macrophages. *J Immunol*. Jul 15 2015;195(2):661-71. doi:10.4049/jimmunol.1401719

40. Burger P, Hilarius-Stokman P, de Korte D, van den Berg TK, van Bruggen R. CD47 functions as a molecular switch for erythrocyte phagocytosis. *Blood*. Jun 7 2012;119(23):5512-21. doi:10.1182/blood-2011-10-386805

41. Oldenborg PA, Zheleznyak A, Fang YF, Lagenaur CF, Gresham HD, Lindberg FP. Role of CD47 as a marker of self on red blood cells. *Science*. Jun 16 2000;288(5473):2051-4. doi:10.1126/science.288.5473.2051

42. Ohira T, Arita M, Omori K, Recchiuti A, Van Dyke TE, Serhan CN. Resolvin E1 receptor activation signals phosphorylation and phagocytosis. *J Biol Chem*. Jan 29 2010;285(5):3451-61. doi:10.1074/jbc.M109.044131
43. Gerlach BD, Marinello M, Heinz J, et al. Resolvin D1 promotes the targeting and clearance of necroptotic cells. *Cell Death Differ*. Feb 2020;27(2):525-539. doi:10.1038/s41418-019-0370-1
44. Rymut N, Heinz J, Sadhu S, et al. Resolvin D1 promotes efferocytosis in aging by limiting senescent cell-induced MerTK cleavage. *FASEB J*. Jan 2020;34(1):597-609. doi:10.1096/fj.201902126R
45. El Kebir D, Gjorstrup P, Filep JG. Resolvin E1 promotes phagocytosis-induced neutrophil apoptosis and accelerates resolution of pulmonary inflammation. *Proc Natl Acad Sci U S A*. Sep 11 2012;109(37):14983-8. doi:10.1073/pnas.1206641109
46. Martin-Rodriguez O, Gauthier T, Bonnefoy F, et al. Pro-Resolving Factors Released by Macrophages After Efferocytosis Promote Mucosal Wound Healing in Inflammatory Bowel Disease. *Front Immunol*. 2021;12:754475. doi:10.3389/fimmu.2021.754475
47. de Bruin AM, Libregts SF, Valkhof M, Boon L, Touw IP, Nolte MA. IFNgamma induces monopoiesis and inhibits neutrophil development during inflammation. *Blood*. Feb 9 2012;119(6):1543-54. doi:10.1182/blood-2011-07-367706
48. Serhan CN. Pro-resolving lipid mediators are leads for resolution physiology. *Nature*. Jun 5 2014;510(7503):92-101. doi:10.1038/nature13479
49. Serhan CN, Savill J. Resolution of inflammation: the beginning programs the end. *Nat Immunol*. Dec 2005;6(12):1191-7. doi:10.1038/ni1276
50. Thorp E, Vaisar T, Subramanian M, Mautner L, Blobel C, Tabas I. Shedding of the Mer tyrosine kinase receptor is mediated by ADAM17 protein through a pathway involving reactive oxygen species, protein kinase Cdelta, and p38 mitogen-activated protein kinase (MAPK). *J Biol Chem*. Sep 23 2011;286(38):33335-44. doi:10.1074/jbc.M111.263020
51. Cai B, Thorp EB, Doran AC, et al. MerTK receptor cleavage promotes plaque necrosis and defective resolution in atherosclerosis. *J Clin Invest*. Feb 1 2017;127(2):564-568. doi:10.1172/JCI90520
52. Kojima Y, Volkmer JP, McKenna K, et al. CD47-blocking antibodies restore phagocytosis and prevent atherosclerosis. *Nature*. Aug 4 2016;536(7614):86-90. doi:10.1038/nature18935
53. Ye ZH, Jiang XM, Huang MY, et al. Regulation of CD47 expression by interferon-gamma in cancer cells. *Transl Oncol*. Sep 2021;14(9):101162. doi:10.1016/j.tranon.2021.101162
54. Levy BD, Clish CB, Schmidt B, Gronert K, Serhan CN. Lipid mediator class switching during acute inflammation: signals in resolution. *Nat Immunol*. Jul 2001;2(7):612-9. doi:10.1038/89759
55. Chiang N, Dalli J, Colas RA, Serhan CN. Identification of resolvin D2 receptor mediating resolution of infections and organ protection. *J Exp Med*. Jul 27 2015;212(8):1203-17. doi:10.1084/jem.20150225
56. Kain V, Jadapalli JK, Tourki B, Halade GV. Inhibition of FPR2 impaired leukocytes recruitment and elicited non-resolving inflammation in acute heart failure. *Pharmacol Res*. Aug 2019;146:104295. doi:10.1016/j.phrs.2019.104295

57. Tourki B, Kain V, Pullen AB, et al. Lack of resolution sensor drives age-related cardiometabolic and cardiorenal defects and impedes inflammation-resolution in heart failure. *Mol Metab*. Jan 2020;31:138-149. doi:10.1016/j.molmet.2019.10.008
58. Maddipati KR. Non-inflammatory Physiology of "Inflammatory" Mediators - Unalamation, a New Paradigm. *Front Immunol*. 2020;11:580117. doi:10.3389/fimmu.2020.580117
59. Hosseini Z, Marinello M, Decker C, et al. Resolvin D1 Enhances Necroptotic Cell Clearance Through Promoting Macrophage Fatty Acid Oxidation and Oxidative Phosphorylation. *Arterioscler Thromb Vasc Biol*. Mar 2021;41(3):1062-1075. doi:10.1161/ATVBAHA.120.315758
60. Sulciner ML, Serhan CN, Gilligan MM, et al. Resolvins suppress tumor growth and enhance cancer therapy. *J Exp Med*. Jan 2 2018;215(1):115-140. doi:10.1084/jem.20170681
61. Spite M, Norling LV, Summers L, et al. Resolvin D2 is a potent regulator of leukocytes and controls microbial sepsis. *Nature*. Oct 29 2009;461(7268):1287-91. doi:10.1038/nature08541
62. Groarke EM, Patel BA, Gutierrez-Rodrigues F, et al. Eltrombopag added to immunosuppression for children with treatment-naive severe aplastic anaemia. *Br J Haematol*. Feb 2021;192(3):605-614. doi:10.1111/bjh.17232
63. Groarke EM, Feng X, Aggarwal N, et al. Efficacy of JAK1/2 inhibition in murine immune bone marrow failure. *Blood*. Jan 5 2023;141(1):72-89. doi:10.1182/blood.2022015898
64. Zeiser R, Polverelli N, Ram R, et al. Ruxolitinib for Glucocorticoid-Refractory Chronic Graft-versus-Host Disease. *N Engl J Med*. Jul 15 2021;385(3):228-238. doi:10.1056/NEJMoa2033122
65. Verstovsek S, Mesa RA, Gotlib J, et al. A double-blind, placebo-controlled trial of ruxolitinib for myelofibrosis. *N Engl J Med*. Mar 1 2012;366(9):799-807. doi:10.1056/NEJMoa1110557

Figure Legends

Figure 1. Cytopenias and BM hypocellularity are associated with increased cell death in SAA. F1 hybrid mice were induced to develop severe aplastic anemia via the radiation followed by splenocyte transfer model. Mice were euthanized 10 days post splenocyte transfer (dpst) and complete blood count data are shown for total WBCs and RBCs (**A**) and platelets (**B**). (**C**) The breakdown of all WBCs is shown. (**D**) Overall BM cellularity in radiation controls and SAA mice. (**E**) Frequency of BM monocytes and neutrophils. (**F**) Absolute number of BM monocytes ($CD11b^+$ $Ly6C^{hi}$ $Ly6G^-$) and neutrophils ($CD11b^+$ $Ly6C^{low}$ $Ly6G^+$). Data shows two pooled independent experiments showing mean ± SEM, n=7-10 per group, significance was determined using a Student's t-test . ** $p<0.01$, *** $p<0.001$, **** $p<0.0001$. (**G**) Gating strategy for AnnexinV and 7-AAD staining to differentiate live, apoptotic, and dead BM cells, plots representative for radiation controls and SAA mice. Numbers reflect the percent of cells within the gated region. (**H**) Frequency of BM cells that are live (open), apoptotic (grey), or dead (black) for both radiation controls and SAA mice days 8 and 10 post splenocyte transfer. Data shows two pooled independent experiments per time point showing mean ± SEM, n=5-10 per group, significance was determined using a Student's t-test . * $p<0.05$, *** $p<0.001$

Figure 2. The expansion of $MerTK^{hi}$ $SIRP\alpha^{hi}$ monocytes and CD47 on apoptotic cells in SAA mice. Mice were induced to develop SAA and BM harvested 10 days post splenocyte transfer (dpst). (**A**) Representative gating for $MerTK^{hi}$ monocytes. Numbers on plots reflect the percent of cells within the gated region. The frequency and absolute number of $MerTK^{hi}$ monocytes is shown in **B** and **C** respectively. (**D**) $SIRP\alpha^{hi}$ staining on $MerTK^{hi}$ monocytes. The frequency (**E**) and absolute number (**F**) of $SIRP\alpha^{hi}$ $MerTK^{hi}$ monocytes. Data represents two pooled independent experiments showing mean ± SEM, n=7-10 per group, significance using a Student's t-test. **** $p<0.0001$. (**G**) Gating strategy for CD47 on live and apoptotic BM cells. Numbers on plots reflect the percent of cells within the gated region. Frequency (**H**) and absolute number (**I**) of CD47 for live

and apoptotic cells. Data representative of one experiment showing mean ± SD, n=3-5 per group. Significance was determined using a Two-way ANOVA with Tukey's multiple comparison test. **** $p<0.0001$.

Figure 3. Enhanced MerTK, SIRPα, and CD47 expression is associated with impaired efferocytosis. (**A**) F1 hybrid mice were induced with SAA and BM harvested 8 dpst. Whole BM was flushed and incubated with PS lipid microparticles for 1 hour at 37°C. (**B**) The lipid microparticles contain attached PS with the phospholipid headgroup exposed and trace amounts of a fluorescent lipid PE-NBD embedded in the particles. (**C**) Representative staining of monocytes and frequency of cells positive for PS-coated microparticles (PS-MPs). Numbers on plots reflect the percent of cells within the gated region. (**D**) Average frequencies of PS-MPs-positive cells among total monocytes. (**E**) Representative staining of macrophages and frequency of cells positive for PS-MPs. Numbers on plots are the percent of cells within the gated region. (**F**) Average frequencies of PS-MPs-positive cells among total F4/80$^+$ BM cells. Significance was determined using a Student's t-test. ** $p<0.01$, *** $p<0.001$.

Figure 4. Imbalanced pro-Inflammatory- pro-resolving lipid mediators. Bone marrow was collected and analyzed by LC-MS/MS. (**A**) Principal component analysis of samples taken from mice without exposure to radiation (healthy), radiation only (RC), or radiation plus splenocytes to induce SAA (SAA) day 3 post-radiation. Each dot represents data from a single mouse and the size of the dot reflects concentration of 18-HEPE. (**B**) Schematic of the biosynthesis of resolvins from ω-3 polyunsaturated fatty acids. Fold change in concentrations of PGD2 (**C**) PGE2 (**D**), or TXB2 (**E**) in the bone marrow of SAA mice, relative to radiation controls (RC), 8 dpst. Data representative of two independent experiments that included 2-3 mice each. Significance was determined using a Student's t-test. * $p<0.05$, ** $p<0.01$.

Figure 5. Exogenous RvE1 improves platelets, BM cellularity and survival. (**A**) SAA-induced F1 hybrid mice were treated with 250ng of RvE1 days 7, 9, 11, and 13 post induction. BM and blood was evaluated day 12 or 14. The breakdown of all WBCs (**B**) and total RBCs (**C**), WBCs (**D**), and platelets (**E**) are shown. (**F**) Total BM cellularity in F1 mice treated with vehicle or RvE1. Absolute number of BM monocytes and neutrophils (**G**), as well as the frequency of LK cells (**H**). Data representative of one experiment per dpst showing mean ± SD, n=5-8 per group. Significance was determined using a Student's t-test. * $p<0.05$. (**I**) Percent survival 30 days post-induction; SAA mice treated with vehicle (solid black line) *n = 18*; SAA mice treated with RvE1 (black dashed line) *n = 19*. Data pooled from three independent experiments.

Figure 6. Exogenous RvE1 improves aberrant monocyte phenotype and efferocytosis. Mice were induced to develop SAA and treated with 250ng RvE1 days 7, 9, 11, and 13 post induction. BM was harvest day 12 or 14 dpst. Representative staining (**A**) and the frequency (**B**) of SIRPα on BM monocytes 14 dpst. Staining (**B** and **D**) and frequency (**C** and **E**) of PS-MPs on monocytes and F4/80^{+} cells 12 dpst, respectively. Numbers on flow plots are the frequency of cells within the gated region. Data from one experiment with mean ± SD, n=5-8 per group. Significance was determined using a Student's t-test. * $p<0.05$

Figure 7. RvE1 therapy reduces SIRPα^{hi} monocytes, increases efferocytosis, and improves resolution. Schematic model illustrating the role of impaired efferocytosis in dysfunctional inflammation resolution and the development of SAA. An increase in SIRPα^{hi} monocytes and CD47^{+} apoptotic cells prevent clearance of apoptotic and dead cells, which is associated with disease progression (left panel). Exogenous RvE1 treatment decreases SIRPα^{hi} monocytes and increases efferocytosis, correlating with improved survival (right panel).

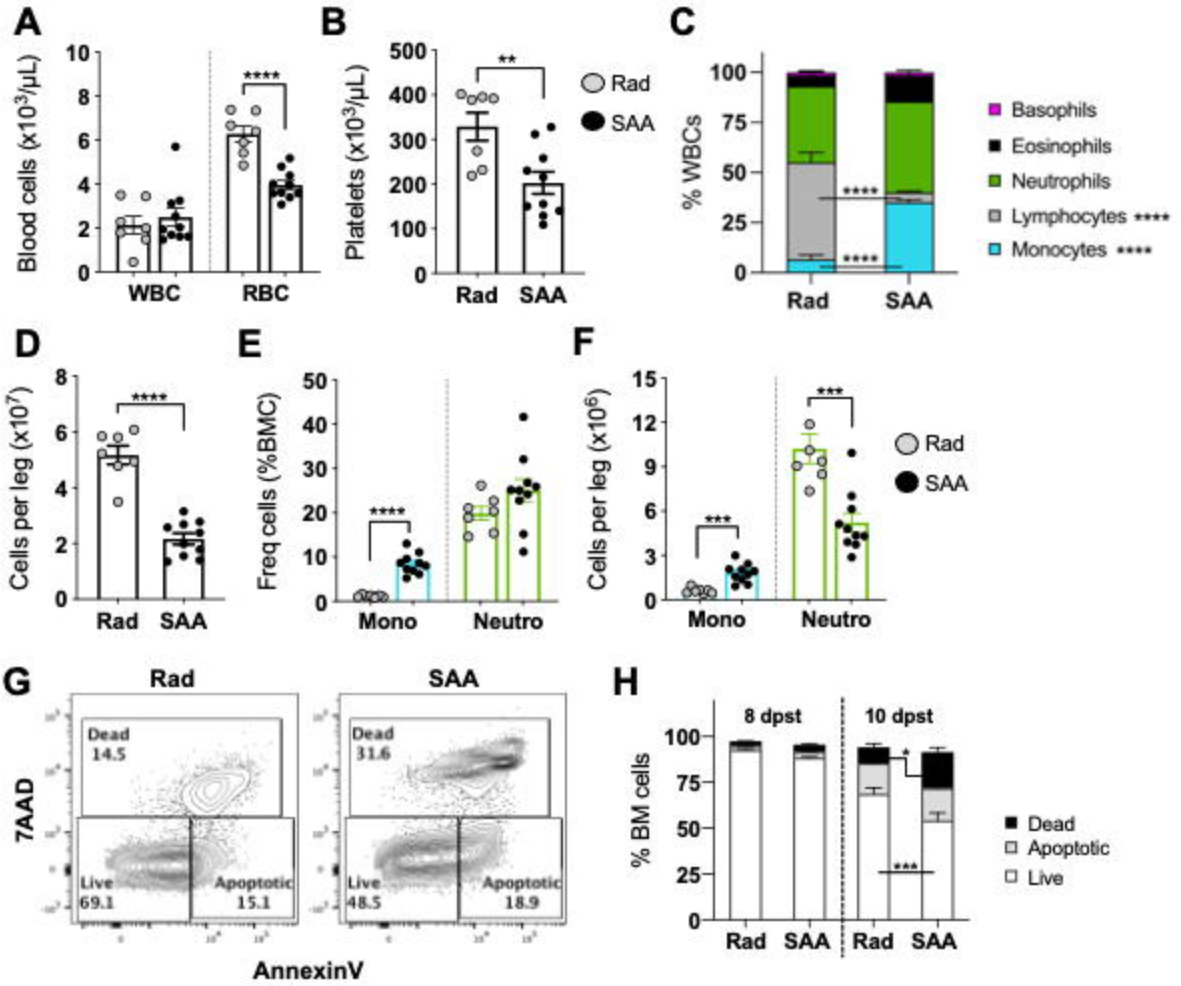
A
Blood cells (x10³/µL)
WBC
RBC
****
B
Platelets (x10³/µL)
Rad
SAA
**
C
% WBCs
Basophils
Eosinophils
Neutrophils
Lymphocytes ****
Monocytes ****
D
Cells per leg (x10⁷)
E
Freq cells (%BMC)
Mono
Neutro
F
Cells per leg (x10⁶)
***
G
Rad
SAA
7AAD
AnnexinV
Dead 14.5
Live 69.1
Apoptotic 15.1
Dead 31.6
Live 48.5
Apoptotic 18.9
H
8 dpst
10 dpst
% BM cells
Dead
Apoptotic
Live

Figure 1

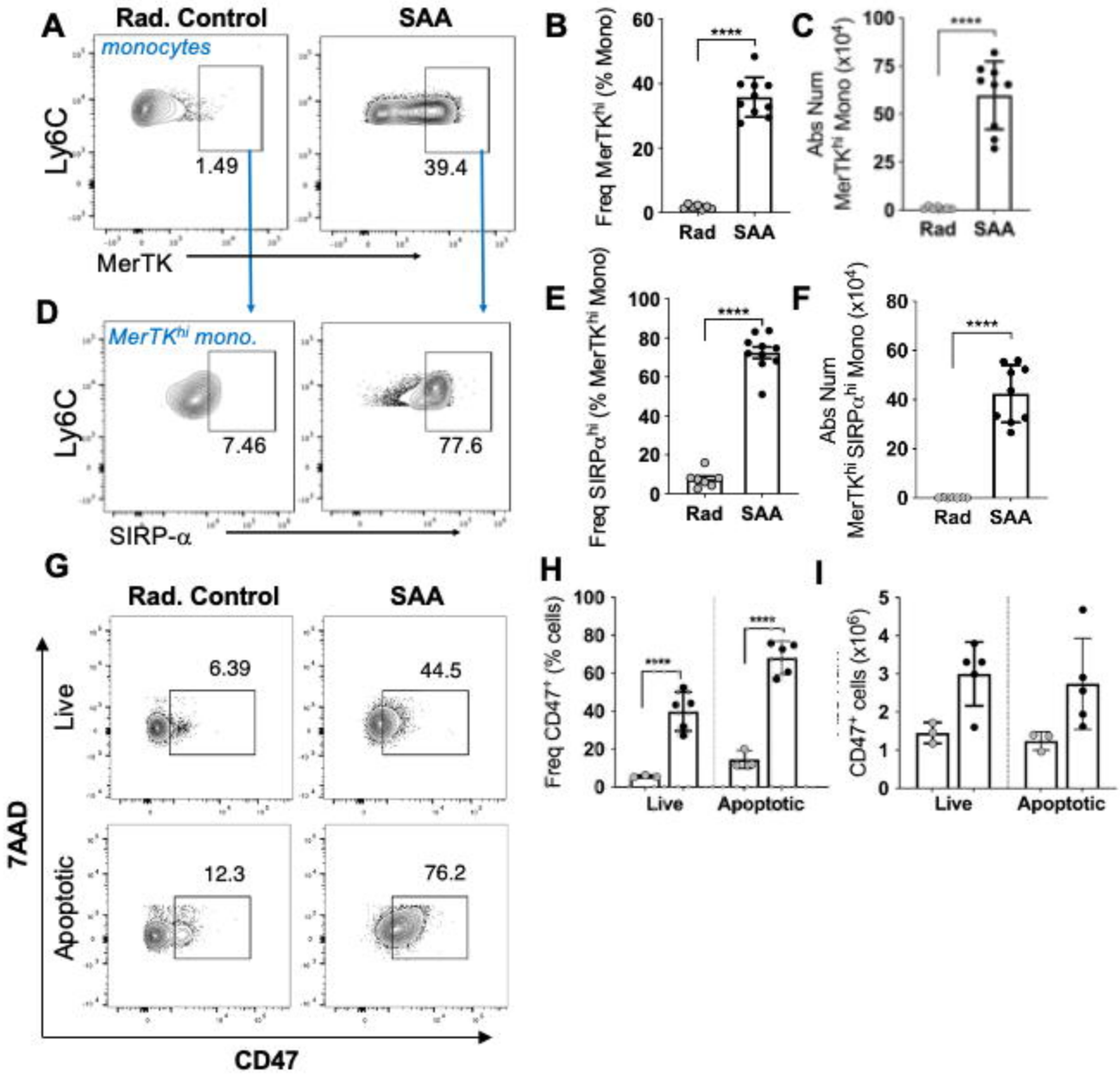
A
Rad. Control
SAA
monocytes
Ly6C
1.49
39.4
MerTK
B
Freq MerTKhi (% Mono)
****
Rad
SAA
C
Abs Num MerTKhi Mono (x10^4)
****
Rad
SAA
D
MerTKhi mono.
Ly6C
7.46
77.6
SIRP-α
E
Freq SIRPαhi (% MerTKhi Mono)
****
Rad
SAA
F
Abs Num MerTKhi SIRPαhi Mono (x10^4)
****
Rad
SAA
G
Rad. Control
SAA
Live
6.39
44.5
Apoptotic
12.3
76.2
7AAD
CD47
H
Freq CD47+ (% cells)
****
****
Live
Apoptotic
I
CD47+ cells (x10^6)
Live
Apoptotic

Figure 2

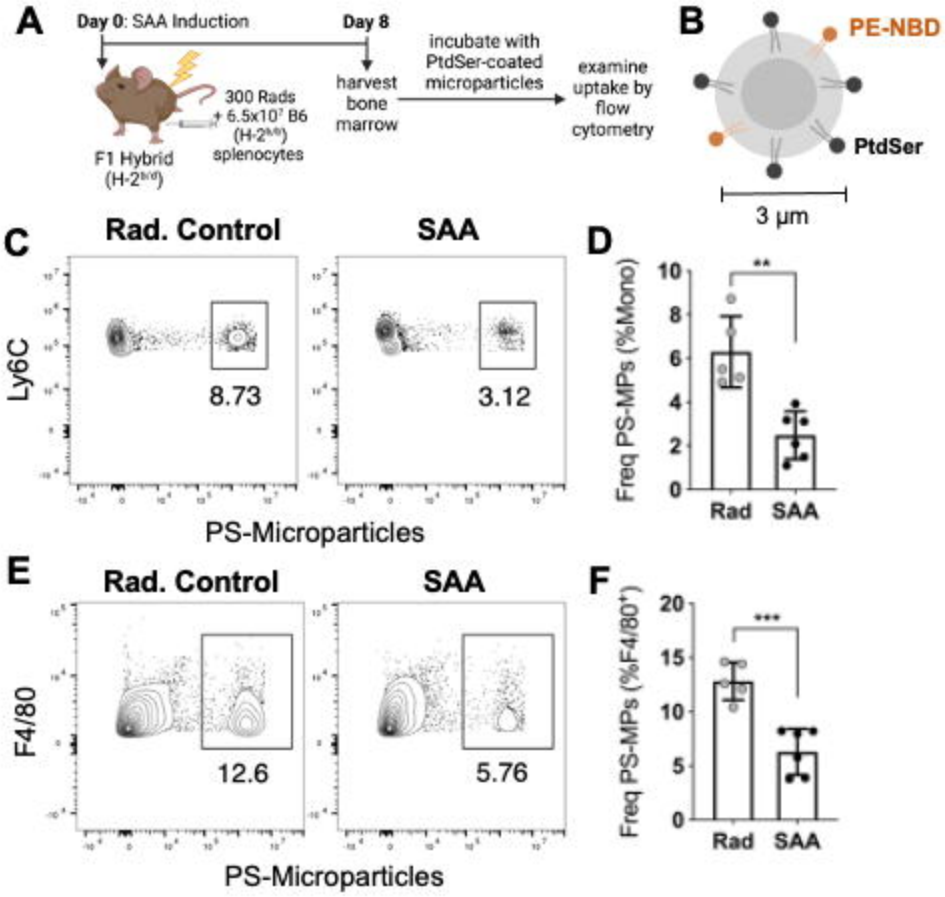
A
Day 0: SAA Induction
Day 8
300 Rads
+ 6.5x10⁷ B6
(H-2b/b)
splenocytes
F1 Hybrid
(H-2b/d)
harvest
bone
marrow
incubate with
PtdSer-coated
microparticles
examine
uptake by
flow
cytometry
B
PE-NBD
PtdSer
3 µm
C
Rad. Control
SAA
Ly6C
8.73
3.12
PS-Microparticles
D
Freq PS-MPs (%Mono)
**
Rad
SAA
E
Rad. Control
SAA
F4/80
12.6
5.76
PS-Microparticles
F
Freq PS-MPs (%F4/80+)
***
Rad
SAA

Figure3

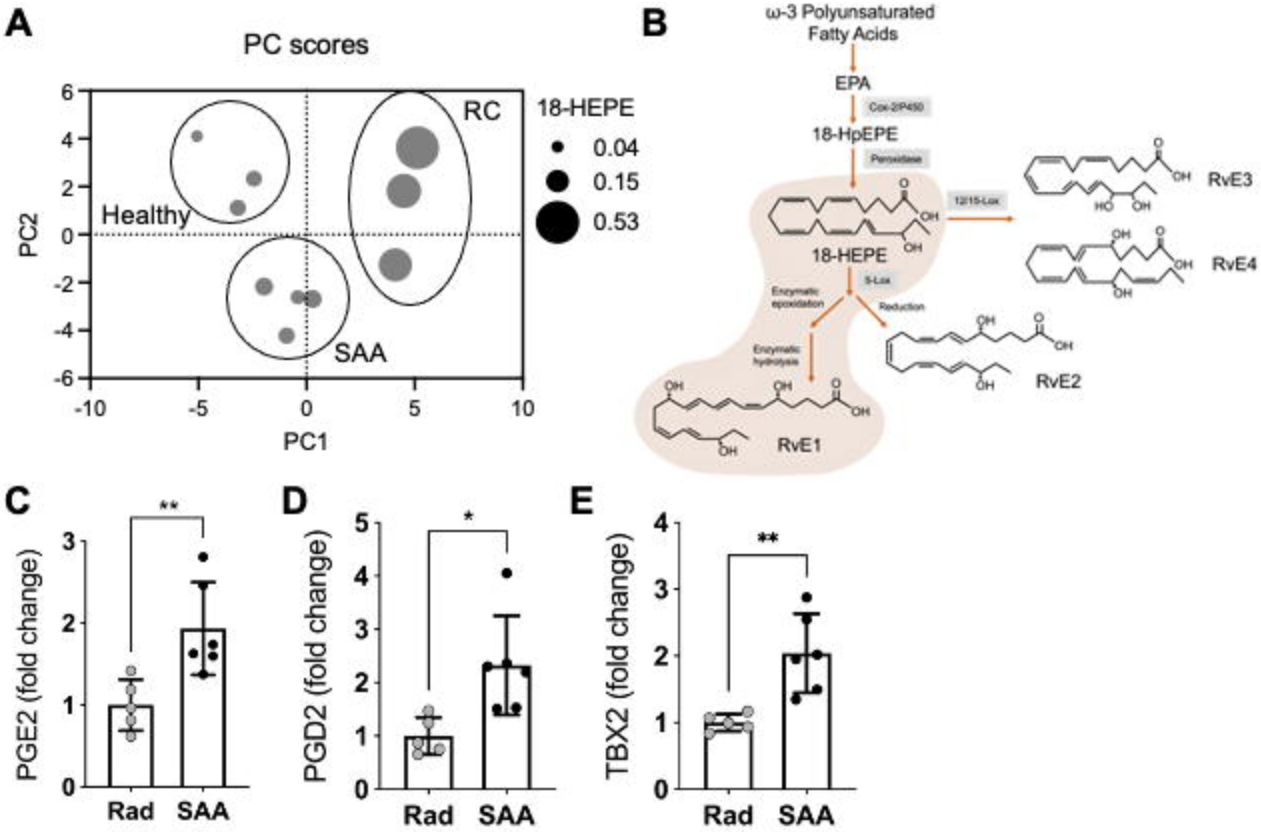
A
PC scores
RC
Healthy
SAA
18-HEPE
0.04
0.15
0.53
PC2
PC1
B
ω-3 Polyunsaturated Fatty Acids
EPA
Cox-2/P450
18-HpEPE
Peroxidase
18-HEPE
12/15-Lox
5-Lox
Enzymatic epoxidation
Reduction
Enzymatic hydrolysis
RvE1
RvE2
RvE3
RvE4
C
PGE2 (fold change)
Rad
SAA
D
PGD2 (fold change)
Rad
SAA
E
TBX2 (fold change)
Rad
SAA

Figure 4

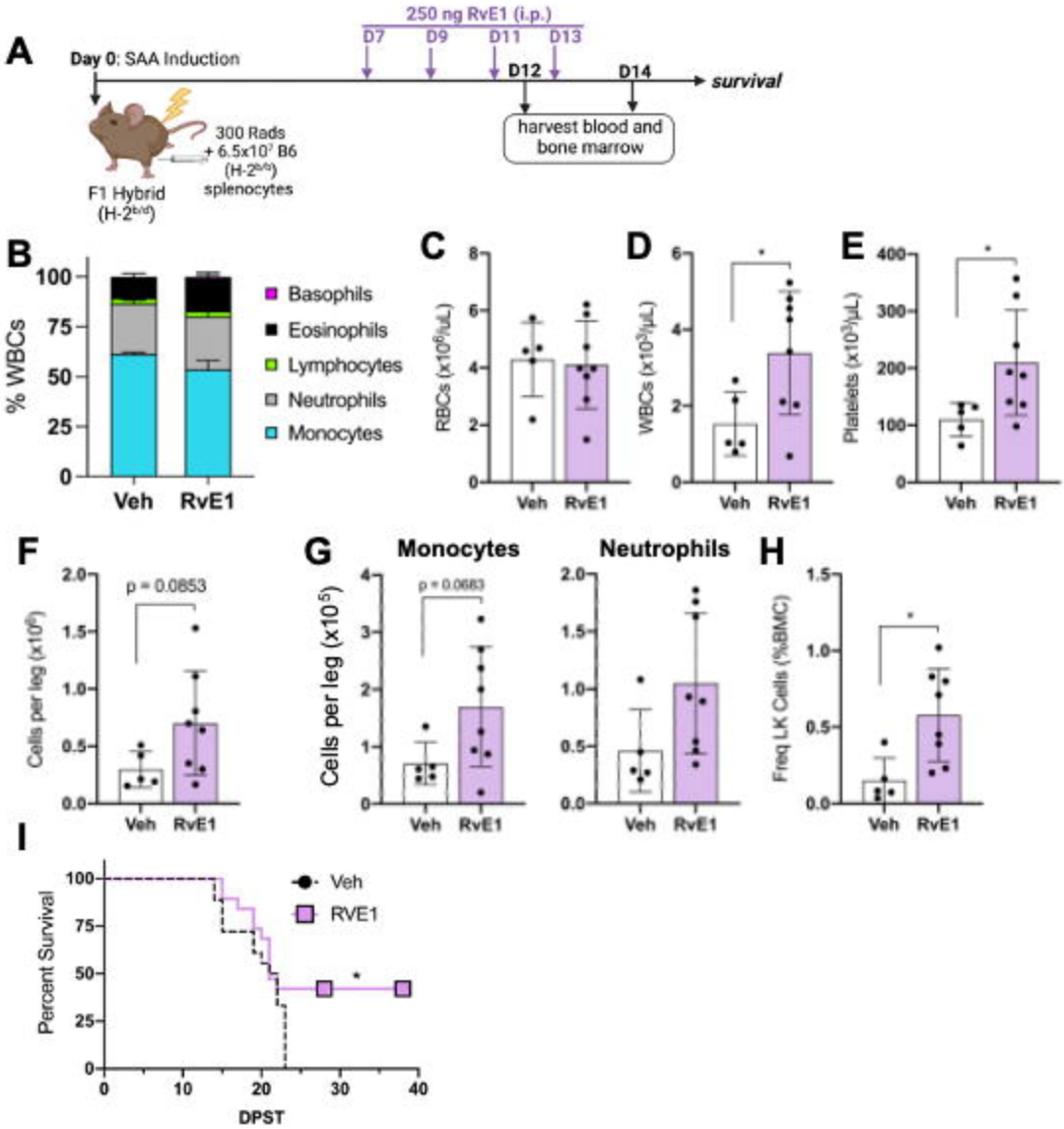
A
250 ng RvE1 (i.p.)
D7
D9
D11
D13
Day 0: SAA Induction
D12
D14
survival
harvest blood and bone marrow
300 Rads
+ 6.5x10^7 B6 (H-2^b/b) splenocytes
F1 Hybrid (H-2^b/d)
B
% WBCs
Basophils
Eosinophils
Lymphocytes
Neutrophils
Monocytes
Veh
RvE1
C
RBCs (x10^6/uL)
D
WBCs (x10^3/µL)
E
Platelets (x10^3/µL)
F
Cells per leg (x10^6)
p = 0.0853
G
Monocytes
Neutrophils
Cells per leg (x10^5)
p = 0.0683
H
Freq LK Cells (%BMC)
I
Percent Survival
Veh
RVE1
DPST

Figure 5

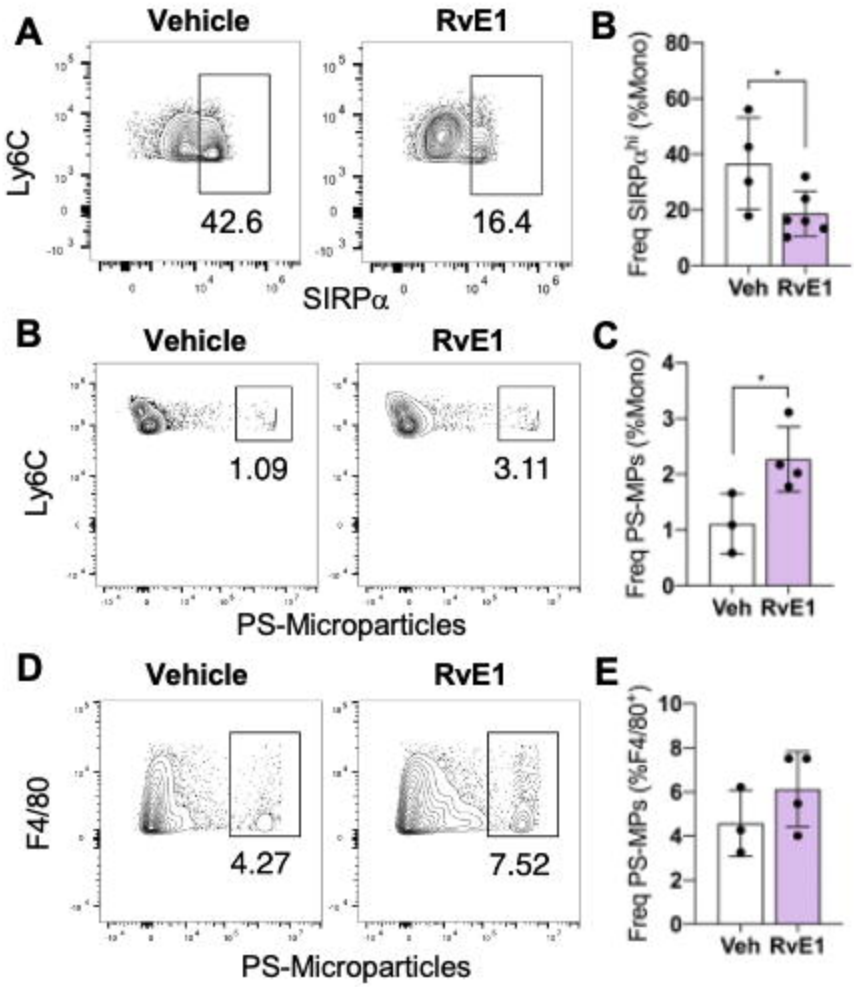
A
Vehicle
RvE1
Ly6C
42.6
16.4
SIRPα
B
Freq SIRPα^{hi} (%Mono)
Veh
RvE1
B
Vehicle
RvE1
Ly6C
1.09
3.11
PS-Microparticles
C
Freq PS-MPs (%Mono)
Veh
RvE1
D
Vehicle
RvE1
F4/80
4.27
7.52
PS-Microparticles
E
Freq PS-MPs (%F4/80$^+$)
Veh
RvE1

Figure 6

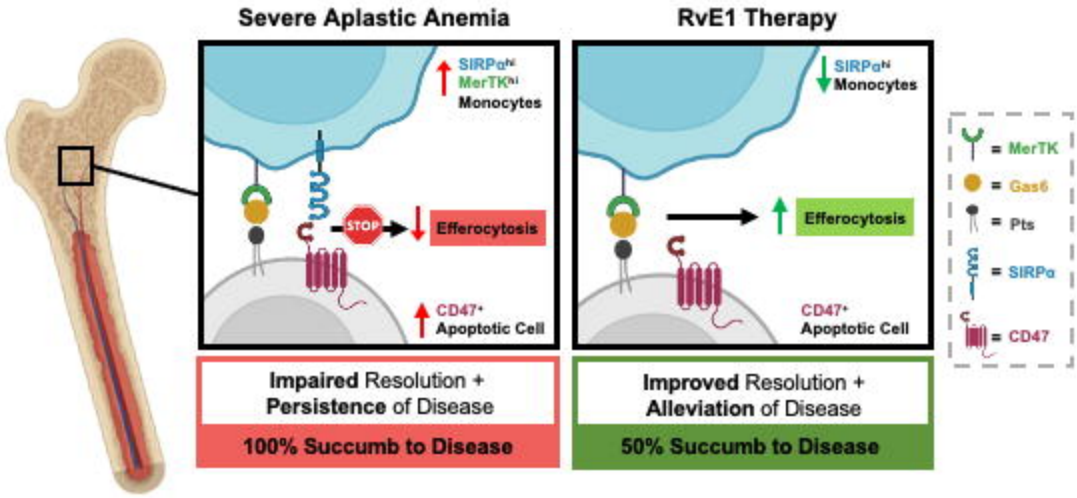
Severe Aplastic Anemia
RvE1 Therapy
SIRPα^hi
MerTK^hi
Monocytes
STOP
Efferocytosis
CD47+
Apoptotic Cell
SIRPα^hi
Monocytes
Efferocytosis
CD47+
Apoptotic Cell
= MerTK
= Gas6
= Pts
= SIRPα
= CD47
Impaired Resolution +
Persistence of Disease
100% Succumb to Disease
Improved Resolution +
Alleviation of Disease
50% Succumb to Disease

Figure 7